

# Ultrafast Structural Evolution of Photoactive Yellow Protein Chromophore Revealed by Ultraviolet Resonance Femtosecond Stimulated Raman Spectroscopy

*Hikaru Kuramochi<sup>† ‡</sup>, Satoshi Takeuchi<sup>†</sup>, Tahei Tahara<sup>\* †</sup>*

<sup>†</sup> Molecular Spectroscopy Laboratory, RIKEN, 2-1 Hirosawa, Wako 351-0198, Japan.

<sup>† ‡</sup> Department of Chemistry and Materials Science, Tokyo Institute of Technology, 2-12-1 Ohokayama,  
Meguro-ku, Tokyo 152-8551, Japan.

E-mail: tahei@riken.jp

## **Supporting information**

1. Experimental
2. Supplementary femtosecond transient absorption data
3. Supplementary UV-FSRS data

# 1. Experimental

## *Materials.*

*Trans-p*-coumaric acid (> 98%) was purchased from Sigma Aldrich and was used as received. It was dissolved in 500 mL of 22 mM phosphate buffer at pH=7 with the solute concentration of 1 mM.

## *Femtosecond transient absorption.*

The details of our femtosecond transient absorption setup have been described elsewhere.<sup>1</sup> Briefly, the output from a Ti:sapphire regenerative amplifier (Legend Elite, Coherent, 800nm, 1 kHz, 1 mJ, 80 fs) was split into two portions. The major portion was used to drive an optical parametric amplifier (TOPAS C, Light Conversion), and the fourth harmonic of the signal light was used as the pump pulse (315 nm, 2  $\mu$ J). The remaining portion was used to generate a white-light continuum by focusing on a CaF<sub>2</sub> plate, which was continuously translated during the experiments to avoid permanent damages. The white-light continuum was then split into the probe and reference pulses. The pump and probe pulses were focused into a 1-mm quartz flow cell (0.5-mm window thickness), in which the pCA solution was circulated. Polarization of the pump pulse was set to the magic angle with respect to the probe pulse. The probe pulse passing through the sample and the reference pulse were collected by fiber bundles, and then introduced into a spectrograph (Chromex 500is/sm) equipped with a CCD camera (TEA/CCD-1024-EM/1 UV, Princeton Instruments). Chirp characteristics of the probe pulse was examined by measuring optical Kerr-effect (OKE) signals of the buffer solution with exactly the same optical configuration, and it was used to correct for the wavelength dependence of the time origin.<sup>2</sup> The pump-probe cross correlation was also estimated by the OKE measurement, and the full width at half maximum (fwhm) of the OKE cross correlation was typically  $\sim 180 \pm 40$  fs with small variations dependent on the probe wavelength.

### ***Ultraviolet resonance femtosecond stimulated Raman spectroscopy (UV-FSRS).***

The setup constructed for the UV-FSRS measurements is shown in Figure S1. The FSRS measurements were carried out by using a combination of actinic pump, probe/reference, and Raman pump pulses.<sup>3-6</sup> To generate these pulses, the output of a Ti:sapphire regenerative amplifier at 800 nm was split into three portions. The first portion was frequency tripled to generate a 267-nm pulse, or was converted to a 300-nm pulse by an optical parametric amplifier and subsequent frequency quadrupling. The generated ultraviolet pulse was used as the actinic pump pulse ( $\sim 2 \mu\text{J}$ ). The second portion ( $\sim 2 \mu\text{J}$ ) was used to generate a white-light continuum in a  $\text{CaF}_2$  plate. The ultraviolet region of the white-light continuum (355 – 405 nm) was spectrally selected and chirp compensated with a pair of fused silica prisms, and it was used as the probe and reference pulses in the Stokes region. The last portion ( $\sim 500 \mu\text{J}$ ) was used to generate the narrow-bandwidth picosecond Raman pump pulse that is tunable in the ultraviolet region. The fundamental pulse at 800 nm was split into two, and they were negatively and positively chirped, respectively, with the same magnitude in grating dispersive lines. These two counter-chirped pulses were sum-frequency mixed in a 5-mm-thick BBO crystal with a crossing angle of  $\sim 2$  degrees, generating a  $\sim 130 \mu\text{J}$ , narrow-bandwidth picosecond pulse at 400 nm.<sup>7</sup> The narrow-bandwidth 400-nm pulse was used to drive a home-built two-stage BBO optical parametric amplifier tuned to 750 nm (or 730, 710 nm), which is seeded by a white-light continuum after a grating-slit spectral filtering. This narrow-bandwidth OPA output was further frequency-doubled, and the generated narrow-bandwidth ultraviolet pulse was used as the Raman pump pulse ( $\sim 15 \text{ cm}^{-1}$ ,  $\sim 1 \mu\text{J}$ , 375, 365, 355 nm). The actinic pump, probe and Raman pump pulses were focused and crossed in a 0.5 mm quartz flow cell (0.5-mm window thickness), in which the sample solution was circulated. Polarization of the pump pulse was set at the magic angle with respect to the other two pulses. The probe pulse passing through the sample and the reference pulse were spectrally analyzed by a spectrograph (iHR-320, Horiba), and their spectra were detected by a pair of photodiode arrays (S3904-1024Q, Hamamatsu). The stimulated Raman gain signal, induced by the Raman pump (and the probe pulse),

was evaluated from the probe and reference spectra by mechanically chopping the Raman pump pulse. The pump-probe cross-correlation of the UV-FSRS measurements was estimated by fitting the temporal profiles of the transient absorption signals in the same wavelength region with a Gaussian instrumental response function. The fwhm value of the cross-correlation was estimated as  $180 \pm 20$  fs. The time origin for each Raman shift was also determined in the same fitting, and the group delay difference of the probe pulse over the present Stokes region was within  $\sim 30$  fs. The frequency resolution of the FSRS measurement is  $\sim 15$   $\text{cm}^{-1}$ .

A typical raw FSRS spectrum of pCA<sup>-</sup> is shown in Figure S2 (A). The raw spectrum contains Raman signals not only from the excited states but also from the ground state, buffer solution, and quartz cell. These additional signals were carefully subtracted with adequate scaling factors (Figure S2 (B)). Then, the sloping background due to the population bleaching of the excited state was modeled by a spline function so that it smoothly connects the wavenumber regions where no band features exist (Figure S2 (C)). Subtracting this modeled background curve, we obtained a pure FSRS spectrum of the excited state as negative absorbance changes (Figure S2 (D)). In the present paper, we represent this FSRS spectrum as a positive stimulated Raman gain in the mOD unit after inverting the sign.

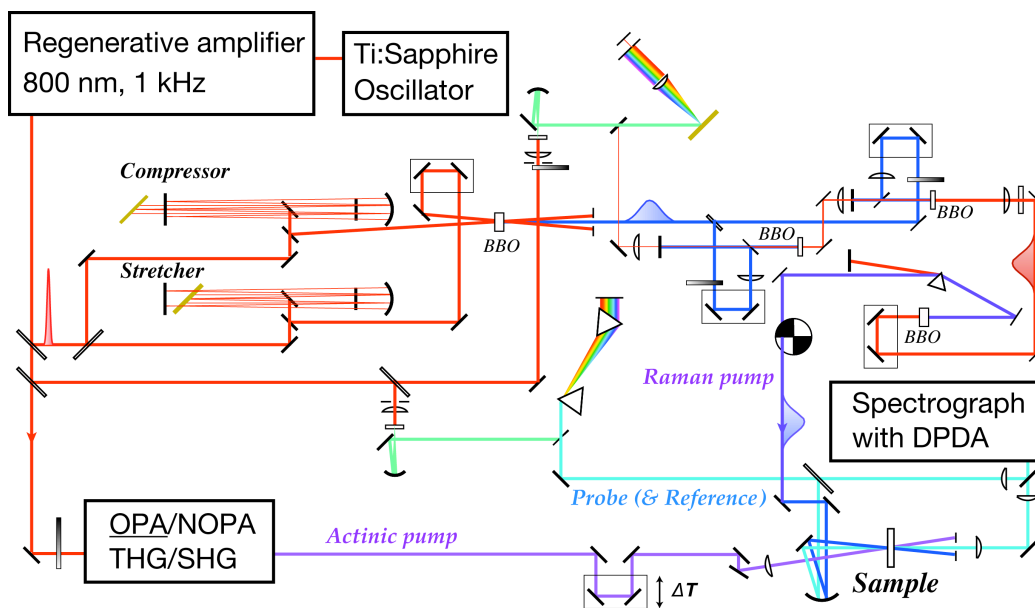


**Figure S1.** Schematic diagram of the UV-FSRS setup.

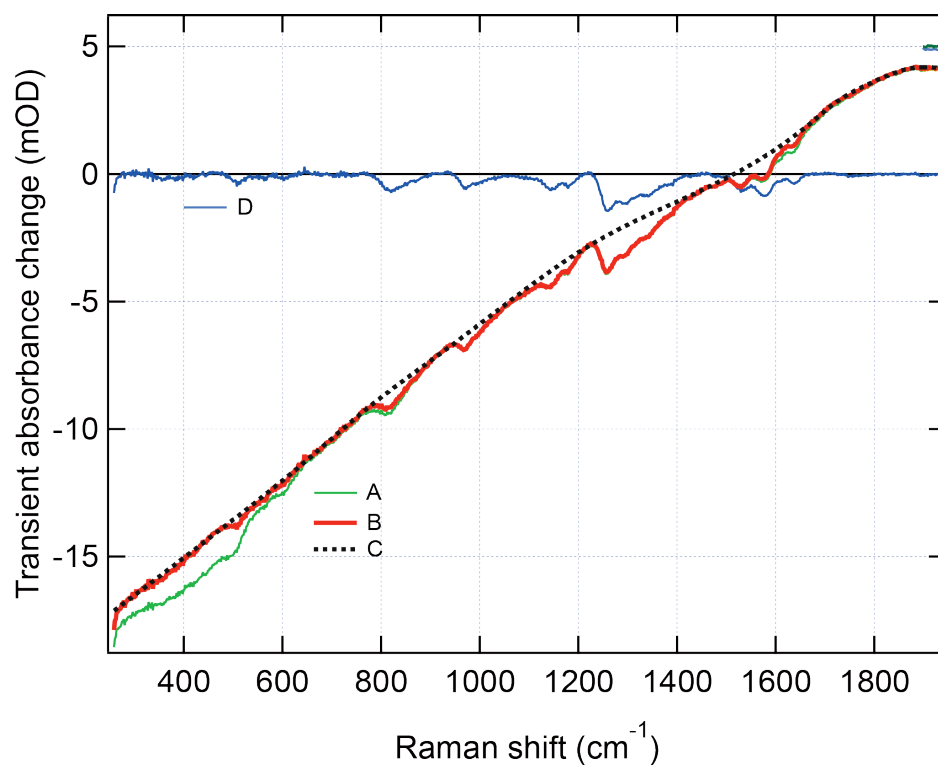


**Figure S2.** Procedure to extract FSRS spectra of the excited state. (A) A typical raw FSRS spectrum of pCA<sup>-</sup> at a delay time of 0.3 ps, (B) The spectrum obtained after subtracting the signals due to the ground state, buffer solution, and quartz cell. (C) A sloping background modeled with a spline curve, (D) The spectrum obtained after subtraction of the sloping background from the spectrum (B).

## 2. Supplementary femtosecond transient absorption data

Temporal profiles of the transient absorption signals at five selected wavelengths are shown in Figure S3. These wavelengths correspond to the blue edge of the excited-absorption band (335 nm), ESA2 maximum (355 nm), ESA1 maximum (375 nm), SE maximum (425 nm), and the isosbestic point between ESA2 and SE (392 nm). The instrumental response function (the instantaneous stimulated Raman gain signal due to the OH stretch mode of water measured at the probe wavelength of  $\sim 353$  nm) is also shown for comparison. It is readily seen that the ESA2 band and SE band decay concomitantly with the 2.5 ps time constant in the time region after 1 ps, as described in the main text. The femtosecond component can be recognized most clearly at the isosbestic point where the ESA2 and SE components are canceled out. In fact, the temporal profile at 392 nm can be successfully fitted with a single-exponential function, giving a decay time constant of  $\sim 250$  fs. This value is significantly shorter than the value obtained from the band integral analysis (450 fs). Because the band integrated intensity only depends on the transition intensity and the population of the relevant electronic state, the 450 fs time constant should be free from spectral shift. The apparent decay time constant at 392 nm becomes shorter than 450 fs due to the substantial shift of the relevant band. In addition, a rising feature can be clearly seen on the femtosecond time scale at the blue edge of the excited-state absorption band, reflecting the ultrafast spectral blue-shift of the transient absorption band. At the Raman pump wavelength (375 nm), a bi-exponential fit of the transient absorption signal gave the 470-fs and 2.5-ps time constants.

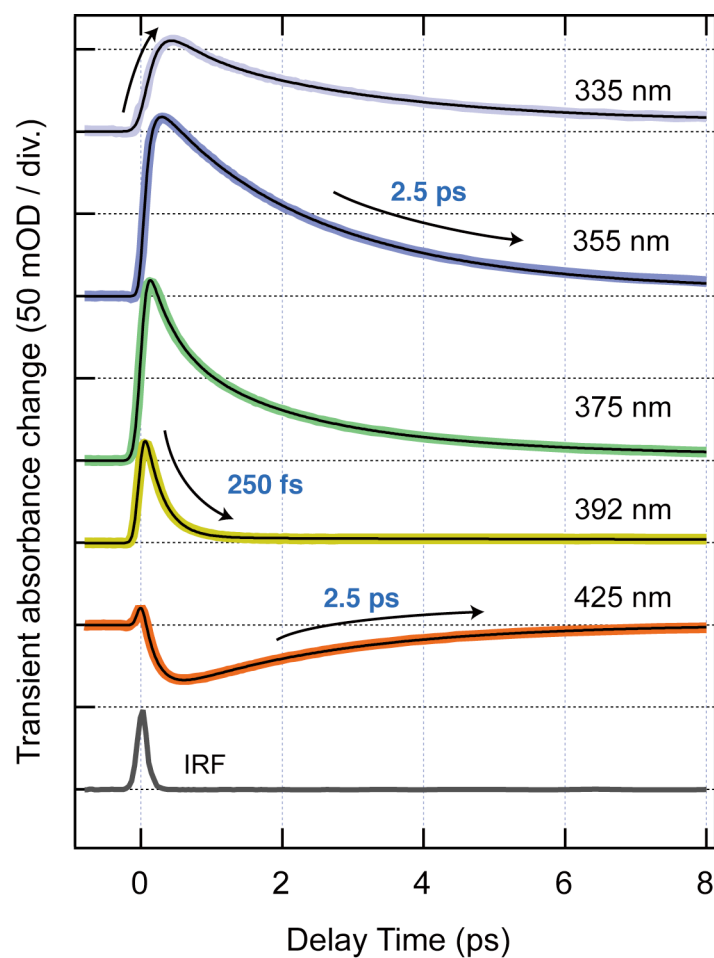


**Figure S3.** Temporal behaviors of the transient absorption signals at five selected wavelengths. Black solid curves represent the best bi-exponential fit. The instrumental response function (IRF) is also shown for comparison.

### 3. Supplementary UV-FSRS data.

In the UV-FSRS measurement, we observed the strongest transient Raman signal in the 1220 - 1450  $\text{cm}^{-1}$  range. This Raman signal exhibits a rather dispersive feature, which is especially pronounced around 1255  $\text{cm}^{-1}$  in the femtosecond time region. As stated in the main text, the Raman pump wavelength (375 nm) is resonant with not only the ESA bands but also the emission band of  $\text{pCA}^-$  (see the steady-state emission spectrum in Fig. 1). This resonance condition can give rise to signals due to an additional third-order optical process using  $S_1 \rightarrow S_0$  resonance,<sup>8</sup> which is different from the stimulated Raman gain process that we basically seek for. This inference is supported by Raman-pump-wavelength dependence of the band shape. As shown in Figure S4, when we tune the Raman pump wavelength away from the SE band region (375  $\rightarrow$  365  $\rightarrow$  355 nm), the dispersive sharp feature around 1255  $\text{cm}^{-1}$  is suppressed, while the spectral feature of the adjacent bands are kept nearly the same. McCamant *et al.* reported a similar behavior, which they called RINE, in other systems where the Raman pump was resonant with the  $S_1$ - $S_0$  stimulated emission band.<sup>8</sup> The intensity of this component is determined by the Franck-Condon factor between the  $S_1$  and  $S_0$  states. Therefore, the observed strong dispersive band shape at 1255  $\text{cm}^{-1}$  suggests that the  $S_1$  and  $S_0$  potential surfaces are significantly displaced along the corresponding mode. According to the ground state Raman spectrum, this mode is highly likely assigned to the in-plane  $\text{C}_{\text{et}}\text{-H}$  bending mode at 1251  $\text{cm}^{-1}$ , indicating that the Franck-Condon molecule starts to distort along the  $\text{C}_{\text{et}}\text{-H}$  bending coordinate. This is consistent with our conclusion that the excited  $\text{pCA}^-$  molecule undergoes ultrafast in-plane deformation from the Franck-Condon state.



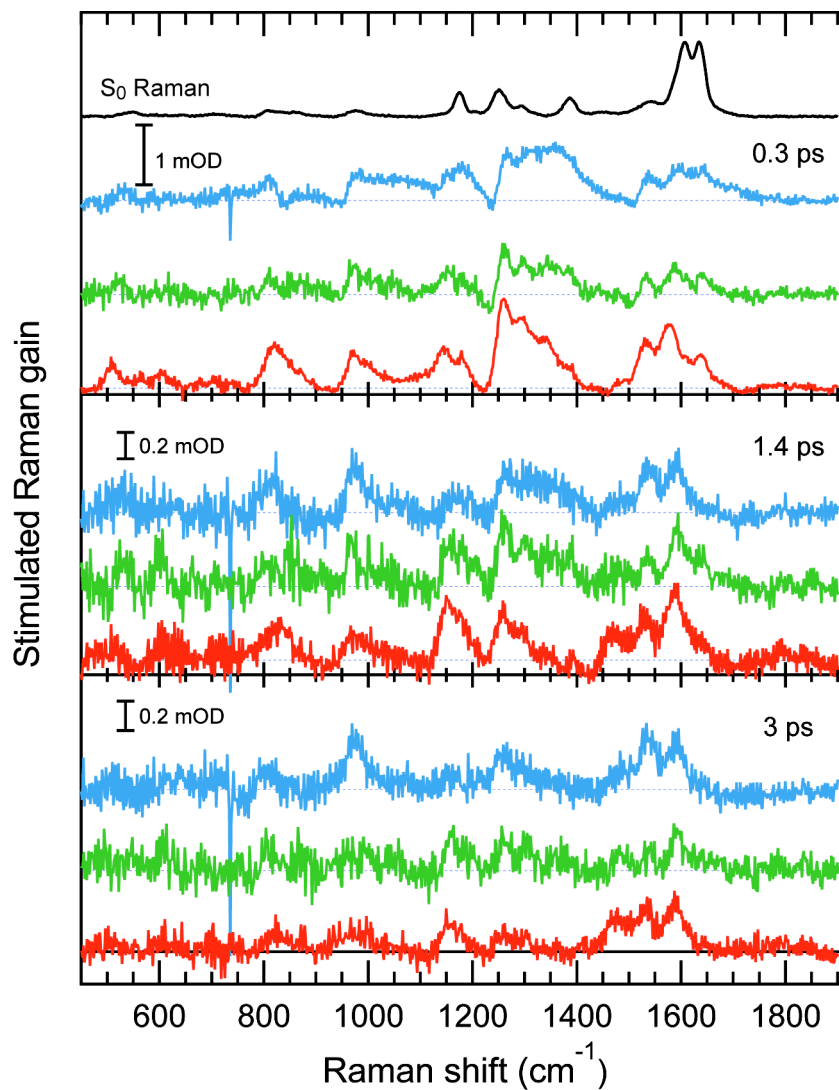


**Figure S4.** FSRS spectra of  $\text{pCA}^-$  at three delay times obtained with three different Raman pump wavelengths: 355 nm (blue), 365 nm (green), and 375 nm (red). The ground-state Raman spectrum is also shown for comparison at the top.

## References

- (1) Iwamura, M.; Watanabe, H.; Ishii, K.; Takeuchi, S.; Tahara, T. *J. Am. Chem. Soc.* **2011**, 7728.
- (2) Yamaguchi, S.; Hamaguchi, H. *Appl. Spectrosc.* **1995**, 49, 1513.
- (3) Yoshizawa, M.; Kurosawa, M. *Phys. Rev. A* **1999**, 61, 013808.
- (4) McCamant, D. W.; Kukura, P.; Yoon, S.; Mathies, R. A. *Rev. Sci. Instrum.* **2004**, 75, 4971.
- (5) Laimgruber, S.; Schachenmayr, H.; Schmidt, B.; Zinth, W.; Gilch, P. *Appl. Phys. B-Lasers O.* **2006**, 85, 557.
- (6) Kovalenko, S. A.; Dobryakov, A. L.; Ernsting, N. P. *Rev. Sci. Instrum.* **2011**, 82, 063102.
- (7) Raoult, F.; Boscheron, A. C. L.; Husson, D.; Sauteret, C.; Modena, A.; Malka, V.; Dorchies, F.; Migus, A. *Opt. Lett.* **1998**, 23, 1117.
- (8) McCamant, D. W.; Kukura, P.; Mathies, R. A. *J. Phys. Chem. B* **2005**, 109, 10449.